

# A Case Study on the Feasibility of RCS Measurements in a Non-Anechoic Environment Using Legacy or Inexpensive Commercial Off-The-Shelf Equipment

C. N. Vazouras, C. Bolakis, E. A. Karagianni, M. E. Fafalios and J. A. Koukos

*Sector of Combat systems, Naval operations, Sea studies, Navigation, Electronics & Telecommunications, Hellenic Naval Academy, Hatzikyriakou Ave., Piraeus 18539, Greece.*

**Abstract.** An experimental setup was built and tested for indoor measurements of Radar Cross Section (RCS) of small targets in the Hellenic Naval Academy (HNA) premises. No anechoic chamber being available, separation of the target echo from unwanted background returns was sought via the old, well-established CW-nulling (CW-cancellation) technique. A simple instrumentation system was implemented along the literature guidelines, with some handy modifications, using a general purpose scalar Spectrum Analyzer (SA) for reception. Several legacy free-floating microwave sources were tested first, achieving cancellation to a limited extent, leaving a residual signal (in the absence of target) with considerable power fluctuations, which, however, can be reduced using the averaging function of the SA. Significant improvement was achieved using an inexpensive Commercial Off-The-Shelf (COTS) phase-locked YIG oscillator which, by careful manual tuning and use of averaging, allows for a fairly stable residual return at levels within 20 dB from the trace-averaged noise floor of the receiver. Further on, calibration measurements with a conducting square plate target at normal incidence were performed, resulting in remarkably close approximation of the established canonical RCS value of the target.

**Keywords:** instrumentation; electromagnetic measurements; radar cross section; CW-nulling; test range; phase-locked frequency synthesizer.

## INTRODUCTION

Measurement of Radar Cross Section (RCS) has been the object of extensive study since the earliest days of radar, initiated in military environments, and began to make its way into the open literature in the 1950s and early 1960s [1]. Modern state-of-the-art measurements [1, 2] usually involve time domain techniques, like gated measurements, and / or inverse FFT data processing, with a high degree of computer control and automation. Such methods require costly special-purpose instrumentation, and, in the indoor case, an appropriate test range (anechoic chamber). On the other hand, an earlier frequency-domain method (i.e. based on monochromatic measurements) may still be applied at incomparably lower cost.

The objective of the present work is to examine the use of the traditional CW-nulling (or CW-cancellation) approach [1-3] with minimal cost and instrumentation requirements. To this end, some range calibration measurements were performed inside the HNA Laboratory Building using readily available legacy equipment of the HNA Telecommunications Laboratory and some inexpensive Commercial Off-The-Shelf (COTS) microwave sources in X-band frequencies. In the absence of a proper indoor test range, namely, in the words of [1], an “enclosure lined with radar absorbing materials” (i.e. an anechoic chamber), as well as time-domain instrumentation, efforts were concentrated upon minimization of the unwanted background echo (i.e. the returns from the test range in the absence of target) via the CW-nulling technique [3-5]. As is well known, the method seeks to (almost) cancel the unwanted echo by subtracting an appropriately attenuated and phase-shift portion of the incident wave. The method dates at least from the early 1950s [4, 5] and probably from the earliest applications of RCS measurements. In [2], as early as 1993, it is referred to as “obsolete”, due to the emergence of swept- and stepped-frequency and time-domain (gated) instrumentation radars, greatly advantageous to speed and efficiency of measurement; as also noted therein, however, the cancellation principle is still applied in newer instrumentation systems. The CW-nulling method is also referenced in the relevant IEEE standard [1]. In short, the method seems to remain as well-established as ever, so long as one recognizes its limitations. It may also be significantly facilitated by some technological and commercial advances, such as the ones exploited in the present study:

- use of a general purpose scalar Spectrum Analyzer (SA) instead of a specialized receiver, taking advantage of its inbuilt digital processing capabilities (unheard of in the early days of the method)
- use of an inexpensive Commercial Off-The-Shelf (COTS) phase-locked frequency synthesizer unit in the X-band as a signal source, to provide the frequency stability indispensable to successful application of the method.

On the other hand, the passive framework of the instrumentation system is very simple and easy to compose, along the well-known guidelines of the literature, using legacy waveguide components. The measurement process is quite cumbersome and time-consuming (as it has always been), but this is the price to pay for the simplicity and inexpensiveness of the instrumentation used. Several preliminary range calibration tests demonstrated the feasibility of considerable reduction of the background echo, implying the possibility of obtaining reasonable RCS estimates for a variety of targets.

## **EXPERIMENTAL SETUP AND INSTRUMENTATION**

A simple experimental instrumentation along the lines of [3-5] was used, as depicted in Fig.1.

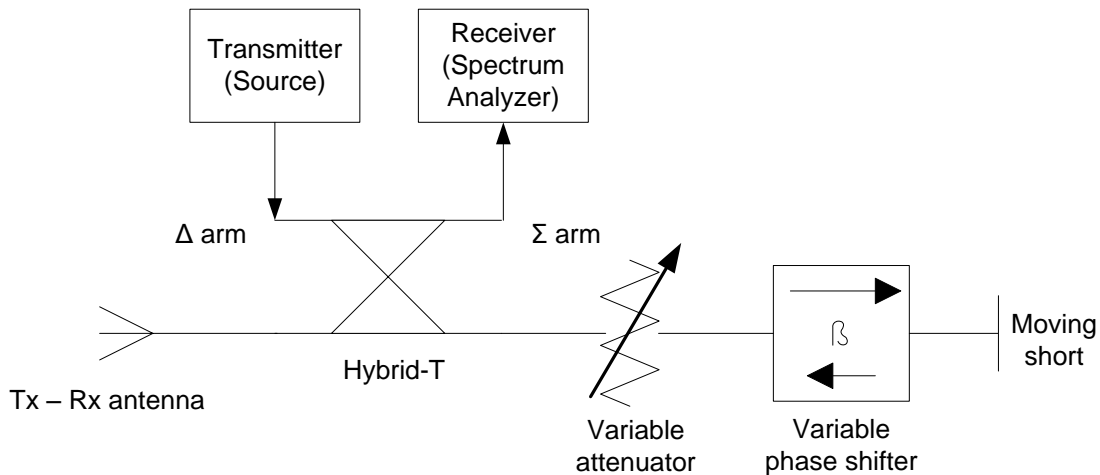


**FIGURE 1.** Block diagram of the measurement instrumentation.

The instrumentation is based on WR-90 rectangular waveguide parts, with the standard inner dimensions of 0.9 in (22.86 mm)  $\times$  0.4 in (10.16 mm) and the recommended frequency band of 8.2 to 12.4 GHz. Referring to Fig.1, the incident wave generated by the microwave signal source is split in halves by means of a magic-T. The first half is transmitted by the antenna, while the second half (out of phase by 180 degrees) travels towards the load via the opposite arm of the magic-T. The signal entering the receiver is proportional to the vector sum of the echo received by the same antenna and the internal reflected wave from the load (a small portion of the second half of the incident wave). As is well known, the CW-nulling technique is based on adjustment of the internal reflected wave to cancel out the background echo at the receiver. In the instrumentation described e.g. in [3-5], a matched load is used and adjustment is achieved by inserting some degree of mismatch by a 3-stub tuner. In the present work, a moving short was used as termination, preceded by a variable attenuator and a phase shifter, both based on the traditional construction of a vane moving across a WR-90 waveguide, with mechanical adjustment using a rotating Vernier scale. To achieve echo cancellation, one adjusts the attenuator and phase shifter to render the magnitude and phase of the internal reflected wave as near the background echo as possible, which results in minimization of the total signal observed at the SA due to the 180 degree phase difference inserted by the magic-T junction. In some cases, moving the position of the shorted termination was also found to be helpful, practically extending the range of phase difference adjustment offered by the shifter.

After testing and comparison with the 3-stub tuner arrangement, the present modified setup appears to achieve a similar or better degree of cancellation, probably due to more precise mechanical adjustment of the attenuator and phase shifter by means of the rotating Vernier. Moreover, by adjusting the attenuator to maximum (about 40 dB), the internal reflected wave is essentially eliminated (attenuated by 80 dB), and hence an estimate of the total background echo level is obtained at the receiver. The adequacy of the attenuation to effectively eliminate the reflected wave in comparison with the background echo was verified by stabilization of the signal at the receiver during the adjustment of the attenuator. Calibration of the system for frequency variation of the transmitter output power and various insertion and reflection losses of the passive components, may be achieved similarly in a simple way by replacing the antenna with a short circuit, eliminating the reflected wave by maximizing the attenuation, and measuring the signal power level at the receiver over the range of frequencies to be tested. The power

variations thus obtained may be subtracted from the actual target echo power levels measured over the same frequency range, to separate the frequency dependency of the target from the one due to the instrumentation system (except the antenna) itself. This, of course, is no system calibration in its proper sense, since it does not take into account the antenna gain and free space losses; as is well known (see e.g. [2]), proper calibration may be achieved via measurements of a “canonical” target such as a conducting plate (at normal incidence) or sphere. However, it is of some interest for initial validation of the present instrumentation system and measurement approach, since it yields an estimate of the frequency behavior of the antenna and target combination, to be assessed by comparison against the expected behavior which for some types of antennas and targets is known to a good degree of accuracy. So, in the following, this procedure will be referred to as “partial calibration”. Further on, setting the attenuator at maximum and replacing the antenna with a power measuring device (a power meter or a spectrum analyzer), we can measure the power fed into the input terminal of the transmitting antenna, i.e. the “available power” for transmission. To get the actual radiated power one should, of course, subtract the mismatch and antenna losses, but they will be taken into account anyway by the “full” calibration procedure. Moreover, the mismatch loss between the waveguide and the antenna is expected to be offset (to a large extent) by the mismatch loss of the waveguide to coaxial adaptor used for the power measurement, which is generally of similar magnitude (e.g., a typical SWR in the range of 1.3 - 1.6 for both). The available power thus measured may be used for comparison of the power output of the various generators tested (and for estimation of the overall system sensitivity).

The antenna used was a WR-90 based pyramidal horn with a gain of approximately 16 dB at 8.2 GHz. A general purpose scalar SA, namely the NS-265 model made by Nex1, was used as receiver. It covers the frequency range 9 kHz – 26.5 GHz, with an amplitude measurement range down to – 110 dBm, an average displayed noise level of – 110 dBm or less, and a frequency flatness of  $\pm 2.2$  dBm at the frequency band of interest (8-10 GHz). Thus, it offers a good (albeit not exceptional) sensitivity and frequency behavior. An input SWR up to 1.5 with an inbuilt 2.92 mm socket is given in the specifications. Our instrument has an inbuilt 7 mm (APC-7) socket (known to outperform the 2.92 mm one in terms of SWR) with an additional N-type adaptor (socket saver); assuming for it a maximum SWR value of 1.3 (typical for good quality N-type connectors), we estimate an overall maximum SWR of about 1.6 for the combination (corresponding to a power reflection coefficient about 0.057 or a mismatch loss of about 0.25 dB). As is typical of most SAs, the accuracy of absolute power measurements is poor (no error limits are even specified by the manufacturer), but comparative results, such as power ratio measurements, are much more reliable. As has already been mentioned, RCS measurements are usually based on such results, deriving absolute RCS values by comparison with measurements of some appropriate “canonical” target. Thus, in the present study, the SA was used to measure received power using the “channel power measurement” function; as it will be seen in the following, only power ratios (in dB) are used for RCS estimation at each frequency. An “adjacent channel power measurement” function is also provided by the SA, measuring power level differences between adjacent frequency ranges (channels), and was used to estimate the distance (in dB) between the received signal level and the corresponding noise floor, as an indication of the achievable dynamic range; to this end, the adjacent channels were set to equal frequency widths (integration bandwidths), located so as to ensure that the received signal lies fully in the first (main) channel and no part of it overlaps with the second (adjacent) channel. To reduce noise, the RF input attenuation was set to zero and the average detection mode was used.

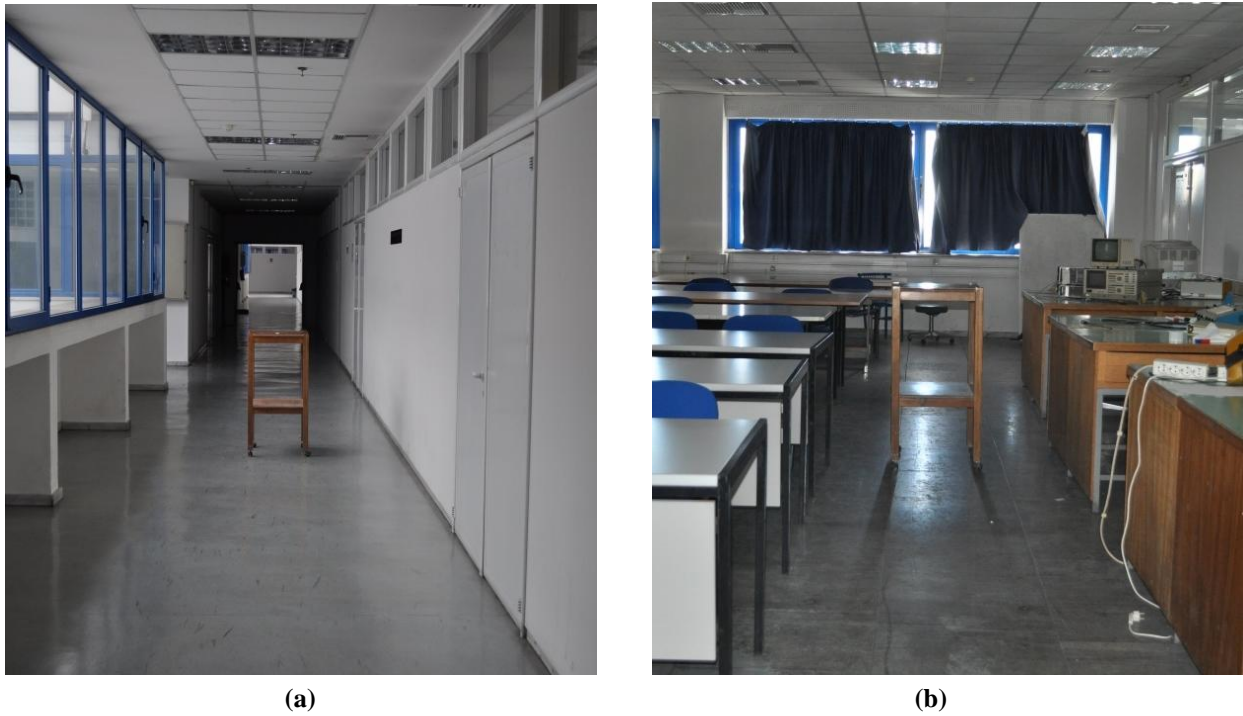


**FIGURE 2.** Test site view: (a) corridor (b) classroom.

In the absence of a proper indoor test range, i.e., in the words of [1], an “enclosure lined with radar absorbing materials”, test measurements were carried out in two indoor sites inside the HNA Laboratory Building: (a) a lengthy corridor (in all about 65 m long, 2.5 m wide and 3 m high), (b) the classroom used by the Telecommunications Laboratory for laboratory exercises and theory lectures (a 15 by 10 by 3 m room, full of furniture and lab equipment). A site view is depicted in Fig. 2. No modification to the usual layout of the sites was made before the test measurements. Both sites, especially the second one, exhibit strong unwanted returns, as expected and verified by the test results. This, in turn, results in serious limitation of the dynamic range and increased uncertainty of measurements. Still, with an appropriate signal source, some useful results may be drawn, as will be seen in the following.

Several microwave signal sources were tested, namely:

- 1) A legacy reflex klystron tube (Raytheon 2K25) oscillator, with an output power typically at 20 – 40 mW (according to various datasheets). Its operating frequency lies between 8.5 – 9.66 GHz, mechanically adjustable by varying the size of the cavity, and electronically adjustable (about 50 MHz around a mechanically adjusted center frequency) by varying the reflector voltage. Voltage feed was provided by a (quite old but recently refurbished and tested) Mid-Century EE/2 power supply. Its reflector voltage ripple does not exceed 3 mV; for the klystron mode used, the frequency shift by reflector voltage is typically around 2-3 MHz per volt, according to the tube specifications, and hence the resulting frequency variation will not exceed a few kHz. The frequency variation due to temperature changes, typically up to about 200 kHz per °C of tube temperature, appears to be a much more important source of frequency fluctuations. A WR-90 isolator with an insertion loss of up to 1.5 dB was used at the tube output for extra frequency stability.

- 2) An old but still fully functional HP 620B (reflex klystron based) microwave signal generator. It operates in the frequency range of 7 – 11 GHz, manually adjustable, with an output power rating at 1 mW minimum. Its typical frequency stability is less than 0.006% per °C of ambient temperature and less than 0.02 % for a 10% line voltage change. A waveguide to coaxial adaptor was used at the generator's N-type output.
- 3) A custom Dielectric Resonator Oscillator (DRO) module built from an extremely inexpensive commercial motion sensor unit, at 10.396 GHz, with a power output of approximately 5 mW measured at the N-type output connector. Limited (about 100 MHz) mechanical tuning is possible but not used here.
- 4) A phase-locked commercial (obtained via surplus sales) frequency synthesizer using an Yttrium Iron Garnet (YIG) tuned oscillator (YTO) unit, namely a Stellex/Endwave MiniYIG 6755-726F unit, attached to a phase-locking controller module by the same provider. The YTO unit is (as all YTOs) electronically adjustable by current tuning, typically up to a recommended value of  $\pm 200$  mA with a 5 MHz/mA sensitivity, i.e. within a  $\pm 1$  GHz frequency range. The center frequency (with zero tuning current) is 9.11 GHz and the power output between 11 – 12 dBm in the 8.1 – 10.1 GHz frequency range, both measured in free-floating mode (without the synthesizer board). In phase-locked mode (with the synthesizer board) the output is programmable at 1 MHz steps, with a power output within 5 – 6 dBm in the above frequency range. The synthesizer module was programmed via serial interface using a Windows PC, according to the instructions found in [6] and [7]; successful locking was verified using the SA. The YTO unit was also tested alone (in free-floating mode) as a signal source, but found to exhibit large short-term frequency fluctuations, similar to the other free-floating sources used (or even larger), attributable to the large temperature drift<sup>1</sup> inherent in the unit (typically  $\pm 30$  MHz and up to  $\pm 60$  MHz). Hence, further such testing was considered uninteresting and not pursued.

All sources were kept idle for an interval of 30 minutes after turn-on, prior to any testing, to allow for temperature stabilization.

## RESULTS AND DISCUSSION

As a first step, testing was carried out for the microwave signal sources (1) – (4) discussed above. For each one of the sources, using the instrumentation setup described in the previous section, the CW-nulling adjustment procedure with no target present was performed, and the received signal, i.e. the residual signal after nulling adjustment, monitored on the SA. A well-known type of instability was exhibited, namely temporal fluctuations of the residual signal power, due to temporal fluctuations of the center frequency of the source, varying substantially across the various sources tested. It was observed, however, that after initial thermal stabilization, there is no significant short-term drift and the frequency fluctuations tend to occur around a more or less stable center frequency. Thus, use can be made of the trace averaging function of the SA in combination with the adjacent channel power measurement function (an example is shown in Fig. 3), to gradually average out the power fluctuations. A significant stabilization of the residual

---

<sup>1</sup> The term “frequency drift” generally means a systematic (non-random) change of frequency with time. In the context of the YTO unit datasheet, however, it denotes just the overall frequency variation with temperature. If the temperature fluctuates, such variations will be observed as temporal fluctuations of the free-floating YTO frequency.

power measurement was thus achieved, depending upon the number of terms (subsequent sweeps) averaged; with 100 or more terms, the power indication was stabilized to within  $\pm 1$  dB of a mean value, taken as the observed value of the residual signal power. The repeatability of the results at time intervals of several minutes was not perfect, ranging within 1 – 2 dB from the previous value for the phase-locked YTO and 3 – 4 dB for the rest of the sources. Such deviations contribute to the uncertainty of target echo measurements, and in practice, with test target echoes at about 30 dB (or more) above the residual power level, as it will be seen in the following, the impact is limited.

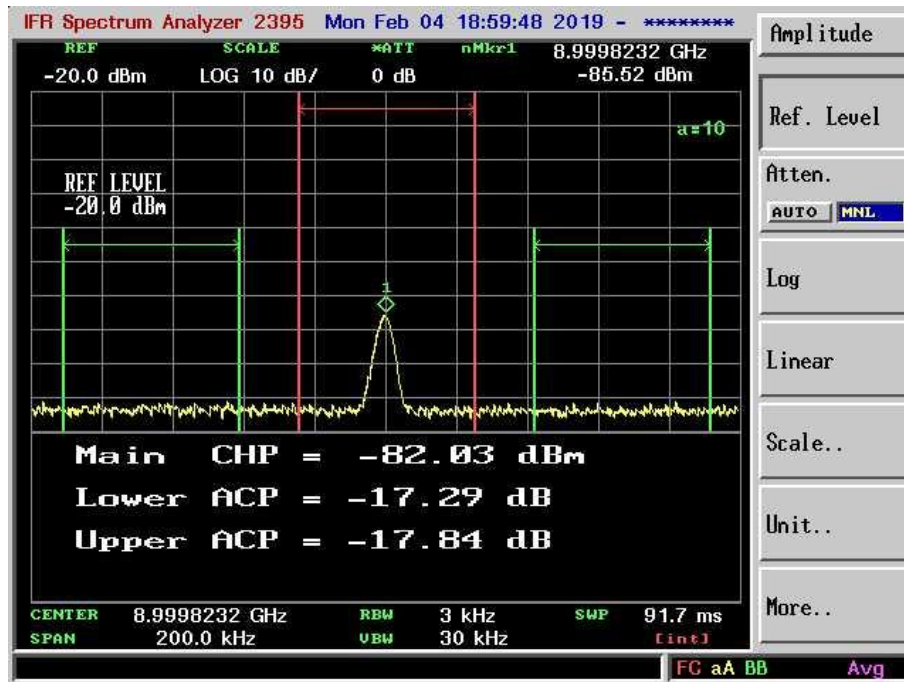


**FIGURE 3.** A spectral view of the residual signal with the phase-locked YTO source.

Upon inspection of the signal power spectrum, some features of each source were deduced:

- The phase-locked YTO source provides, as expected, the best signal in terms both of bandwidth (or, otherwise stated, phase noise) and of fluctuations. A 100 kHz frequency span was used for adjacent channel power measurements, with the default values (automatically adjusted by the SA) of 3 kHz for the resolution bandwidth (RBW) and 30 kHz for the video bandwidth (VBW). The indication of the signal's 20-dB bandwidth with this RBW was approximately 10 kHz. Upon reduction of the RBW it diminishes, in accordance with the measured results shown in [6] and the phase noise specifications of the YTO. However, a smaller RBW value was not adopted, partly to avoid large sweep times and partly because, with a finer RBW, the inherent limitations of the onboard reference temperature compensated voltage controlled crystal oscillator (TCVCXO) of the synthesizer (noticed in [6]) are expected to become apparent, exhibiting smaller-scale frequency instabilities which would complicate the measuring process without significantly altering the averaged results. With the RBW used, the short-term frequency fluctuations within the time required for trace averaging were almost invisible. At significantly larger time intervals, a slower fluctuation up to about  $\pm 50$  KHz around the

center frequency was sometimes observed; it might be attributed to small frequency instabilities of the reference TCVCXO and / or small temperature fluctuations in the YTO. It was generally not fast enough to disrupt the averaging process, but in some cases required repetition of the nulling adjustment before target echo measurement.

- The HP 620B signal generator exhibits significant frequency fluctuations of about  $\pm 100$  kHz around the center frequency. A 1 MHz frequency span was adopted for the SA measurements, with the default values of 10 kHz RBW and 100 kHz VBW. The indication of 20-dB signal bandwidth with this RBS is near 50 kHz.
- The 2K25 reflex klystron oscillator exhibits the strongest frequency fluctuations, up to about  $\pm 500$  KHz around the center frequency, and correspondingly strong residual power fluctuations. The frequency span of the SA was set to 5 MHz, with the corresponding default values of 30 kHz RBW and 300 kHz VBW, and the 20-dB signal bandwidth indication was also inferior to the previous source, of the order of 250 kHz or so; in both cases, precise observation of the 20-dB bandwidth was difficult due to frequency fluctuations.
- The DRO oscillator exhibits smaller frequency fluctuations of about  $\pm 50$  KHz around the center frequency, but a very large phase noise. With a 5 MHz frequency span setting, as above, the 20-dB signal bandwidth is indicated at about 2 MHz; we believe it to be the main reason for the inferior performance observed for this source, as will be seen presently.

Besides the residual return signal, the background echo power and the available power for transmission were also measured in the manner described previously. Due to much larger values and the very nature of these quantities, no significant instability problem was encountered. The results for the worst-case classroom site are shown on Table 1. The 1 dB compression point of the SA is at  $-10$  dBm, indicating that all measurements are well within the dynamic range of the instrument; the same is true of measurements presented in the following.

**TABLE 1.** CW-nulling adjustment test results for various microwave signal sources

Microwave Signal Source	Frequency (GHz)	(1) Residual Power After Nulling (dBm)	(2) Background Echo (dBm)	(3) Available Power (dBm)	Margin (dB) (3) – (1)
2K25 reflex klystron	9.000	-72	-23.5	-1.5	70.5
HP 620B generator	9.000	-80	-47	-16	64
DRO module	10.396	-66	-51	-9.2	56.8
Phase-locked YTO synthesizer	9.000	-82	-34.5	-4	78

For the corridor site, similar tests were also performed, yielding consistently improved (i.e. lower) values of background echo power by 4 – 5 dB, and of residual signal power by 2 – 3 dB. The improvement may be attributed to the length of the corridor, as well as the absence of diverse scatterers like furniture and equipment. Thus, calibration measurements with a canonical target, as will be presented in the following, were carried out in the corridor site.

The margin between the available power and the residual power, essentially the quantity defined in [3] (Sec. 11.5.1.1) as isolation between transmitter and receiver, may be used for comparison of the “nulling efficiency” of the various sources. The value achieved with the YTO

source seems remarkably good, especially in the corridor site (cf. Table 2 below), even though it still falls short of the order of 100 dB recommended in [3] for accurate measurement of target nulls. On the other hand, the background echo power obviously gives an indication of the noisiness of the test site's environment, corresponding to each source; different sources resulted in different levels of background echo. A more clear comparison could also use the margin between the background echo power and the available power level. Both figures of merit may seem somewhat superfluous in the present case, since the superiority of the phase-locked YTO source is already clear from the preceding discussion (and actually was expected from the beginning), but provide some additional quantitative insight.

We finally note that a wooden table (visible on Fig. 2) was used as a handy bearing, and found to increase the background echo by approximately 0.5 dB, but with a negligible effect on the residual power, i.e. successfully eliminated by the nulling adjustment. For future RCS measurements, construction of a polystyrene foam bearing with a simple positioning setup is envisaged.

Following the preliminary tests described above, a series of target return power measurements were carried out in the corridor site, using the YTO synthesizer, within a frequency range of 8.4 – 9.6 GHz. The target was a square aluminum plate of  $30.5 \times 30.5$  cm dimensions, located at a distance of 6 m, at normal incidence. As is well known [2], such a plate may serve as an appropriate calibration target, with an RCS value known to a good degree of accuracy, given by the physical optics approach (see e.g. [2], eq. 5.22)

$$\sigma = 4\pi \frac{A^2}{\lambda^2} \quad (1)$$

where  $A$  is the physical area of the plate, i.e.  $A = d^2$  for a square plate, with  $d$  the side length.

In the case of measuring the RCS of a practical target, these would be the calibration measurements, taken as reference values to comparatively estimate the RCS of the target of interest. In the scope of the present study, however, our goal is to assess the possibility of estimating the known RCS value of the square plate target via measurements by the present instrumentation in rather unfavorable conditions. To this end, the corresponding “partial calibration” procedure (as defined previously) was employed, and the signal power  $P_{c,meas}$  at the receiver upon replacing the horn antenna with a waveguide short was measured besides the actual return power at all frequencies involved. We also denote

- the power output of the signal source by  $P_s$
- the available power for transmission (as defined previously), i.e. approximately the power fed to the terminal of the transmitting antenna, by  $P_t$
- the echo power inwards at the same point, now viewed as the output of the receiving antenna, i.e. the power extracted from the terminal of the receiving antenna, by  $P_r$
- the return power measured at the receiver by  $P_{r,meas}$

The measurement results (in dBm) are tabulated in Table 2. In all cases, the residual return power levels were no more than 20 dB above the trace-averaged noise floor of the receiver (as indicated by the adjacent channel power measurement of the SA). It is worth noticing that levels of return power significantly below the background echo levels are easily detected and measured, of course due to the low levels of residual power achieved by the nulling adjustment.

**TABLE 2.** Measurement results for a square plate target (all powers in dBm)

Frequency (GHz)	Residual Power	Background Echo	$P_{r,meas}$	$P_{c,meas}$
8.4	-88	-47	-55.5	-12.3
8.6	-90	-51	-54.5	-12.7
8.8	-85	-37	-52	-10.7
9.0	-85	-39	-53.5	-10.3
9.2	-87	-36.5	-53.5	-13.1
9.4	-92	-35	-51	-13.3
9.6	-85	-41.5	-52	-13.3

Since the reflection coefficient of the waveguide short equals 1 to a good degree of accuracy, it may be safely assumed that, upon replacing the horn antenna with a waveguide short, the power  $P_t$  is totally reflected inwards and we can write

$$P_{c,meas} = P_t - L \quad (2)$$

$$P_{r,meas} = P_r - L \quad (3)$$

where all powers are in dBm and  $L$  (in dB) is the total loss along the signal path from the output of the receiving antenna to the receiver (including insertion and reflection losses of the components involved, the impact of power splitting by the hybrid-T etc.)

From (2) – (3) it follows that

$$P_r - P_t = P_{r,meas} - P_{c,meas} \quad (4)$$

Eq. (4) allows estimation of the difference between  $P_r$  and  $P_t$  via the difference between the measured quantities  $P_{r,meas}$  and  $P_{c,meas}$ , which incorporate the corresponding internal losses of the instrumentation. On the other hand,  $P_r$  and  $P_t$  are related via the radar range equation (see e.g. [2]), which, with the same antenna for transmission and reception, in its simplest form is

$$P_r = P_t' \frac{G^2 \lambda^2 \sigma}{(4\pi)^3 R^4} \quad (5)$$

or, in logarithmic form

$$P_r' - P_t' = 2G + \sigma + 20 \log(\lambda/R^2) - 30 \log(4\pi) \quad (6)$$

In (5-6), the primed quantities denote the transmitted and received power at the horn antenna, after mismatch loss (both for transmission and reception) at the antenna terminal. To account for this loss, denoted by  $L_A$  (in dB), we write

$$P_t' = P_t - L_A \quad (7)$$

$$P_r = P_r' - L_A \quad (8)$$

and hence

$$P_r - P_t' = P_r - P_t + 2L_A = P_{r,meas} - P_{c,meas} + 2L_A \quad (9)$$

Upon combining (4) and (9), the experimental RCS of the target is estimated via

$$\sigma = P_{r,meas} - P_{c,meas} + 2L_A - 2G - 20 \log(\lambda/R^2) + 30 \log(4\pi) \quad (10)$$

where the power values are in dBm, the transmitting and receiving antenna gain  $G$  is in dB,  $R$  and  $\lambda$  are in meters and  $\sigma$  is in dBsm (dB square meters). For the gain  $G$ , a typical variation of roughly 0.6 dB per GHz across the X-band frequencies (as e.g. in [8], Sec. 13.4) was used. For the mismatch loss  $L_A$ , a reasonable estimate may be obtained by a SWR value of 1.3. For WR-90 waveguide horn antennas with a waveguide to coax adaptor, maximum values of SWR at 1.3 or less (e.g. 1.25) according to datasheets are not unusual; in our setup, no waveguide to coax

adaptor (which tends to increase mismatch losses) is present. Thus, with an antenna  $SWR = 1.3$ , the corresponding mismatch losses are  $2 L_A \cong 0.15$  dB.

As regards the measurement uncertainty, a simple and rough estimate may be obtained based on the observation that the procedure described here is essentially a power ratio measurement, as is also apparent in (10). Both power measurements involved ( $P_{r,meas}$  and  $P_{c,meas}$ ) were carried out at the same frequency and with the same configuration of the measuring instrument (the SA). Thus, most instrumentation uncertainties do not affect the total uncertainty, while others (such as the  $\pm$  half-count error) are significantly small in magnitude, as noted e.g. in [9, 10]. Further on, as also discussed and visualized in these classical references, the largest source of uncertainties is by far the mismatch uncertainties, due to generator and load mismatches along the signal path. In our instrumentation setup, reasonable estimates for these mismatches, as mentioned previously, are:

- Load  $SWR \cong 1.6 \Rightarrow$  Load reflection coefficient  $\rho_L \cong 0.23$  (as discussed for the SA)
- Generator  $SWR \cong 1.5 \Rightarrow$  Generator reflection coefficient  $\rho_g \cong 0.2$  (a conservative estimate for the waveguide to coaxial adaptor used to connect the YTO generator)

In a simplistic first approach, we may use the (rather conservative) traditional worst-case approach outlined in [9, 10], while neglecting possible instrumentation uncertainties for the quantity ( $P_{r,meas} - P_{c,meas}$ ) and focusing on mismatch uncertainties. A more rigorous and detailed examination and statistical treatment along the guidelines of ISO 17025 (as outlined e.g. in [10]) is envisaged for future test measurements. Further sources of error, besides mismatch uncertainties, include

- the antenna gain  $G$
- the residual unwanted echo power, say  $P_{res}$ , after CW-nulling
- the mismatch loss  $L_A$

All of the above factors correspond to the traditionally termed “systematic” errors; a “random” error component should be added. (In ISO 17025 terms, these two concepts are replaced by “Type B” and “Type A” uncertainties, but with no strict correspondence meant.)

For the mismatch uncertainties, the uncertainty boundaries are given by

$$M_{u,max} = 10 \log(1 + \rho_g \rho_L)^2 \cong 0.39 \text{ dB} \quad (11)$$

$$M_{u,min} = 10 \log(1 - \rho_g \rho_L)^2 \cong -0.21 \text{ dB} \quad (12)$$

The above uncertainty contributions must be doubled, since two power measurements are involved, amounting to a total  $+0.78$  to  $-0.42$  dB contribution.

The uncertainty in the antenna gain  $G$  turns out to be quite important, since this (lacking a calibrated reference antenna) was obtained by two power measurements using a HP 432A power meter with a HP 8478B thermistor mount. The measurement conditions are close to those adopted for the detailed example given in [9] and [10], minus the reference oscillator error (not existing for the thermistor sensor) which is approximately offset by the larger instrumentation error margin of the HP432A ( $\pm 1\%$  instead of  $\pm 0.5\%$  full-scale). We also adopt a more conservative estimate for the load mismatch loss, using the maximum  $SWR = 1.35$  of the sensor specifications, instead of the typical one of about 1.15 at the frequency of interest or the 1.2 value used in the example. This results in an increase of about 0.1 dB in the mismatch uncertainty margins with regard to the example values; in all, following the example of [9,10] with these modifications and rounding up to first digit, we obtain a worst-case uncertainty estimate of approximately  $\pm 0.5$  dB for each power measurement, i.e. a total of  $\pm 1$  dB for the antenna gain  $G$ .

The residual echo power after nulling, as already noted, adds directly to the total uncertainty, since there is no phase correlation with the wanted return signal. Denoting it by  $P_{res}$ , the upper and lower error bound due to this term may be written as

$$R_{u,max/min} = 10 \log \left( 1 \pm \frac{P_{res}}{P_{r,meas}} \right) \quad (13)$$

As seen in Table 2, the largest (worst-case) value of  $P_{res}$  is about 31.5 dB below the corresponding measured return power  $P_{r,meas}$ , which yields a very small  $R_u$  contribution of  $\pm 0.0031$  dB. (Even a residual value at 20 dB below  $P_{r,meas}$  would give only about  $\pm 0.044$  dB).

Further on, the uncertainty contribution from  $L_A$  may be neglected due to the small value of  $L_A$  itself; in other words, it is covered by the value of generator SWR  $\cong 1.5$  adopted here. Finally, the “random” error component may be estimated at roughly  $\pm 1$  dB, since this was the range of fluctuations of the power indication around its mean (measured) value, as noted previously.

Adding up the above contributions and rounding up to first digit, a total worst-case uncertainty estimate of approximately +2.8 to -2.5 dB is obtained. An additional (not accounted for) source of errors is the antenna – target misalignment (deviation from normal incidence), possibly in the range of several degrees (due to manual alignment), even though before every measurement an alignment of the target was carried out to the position maximizing the received signal.

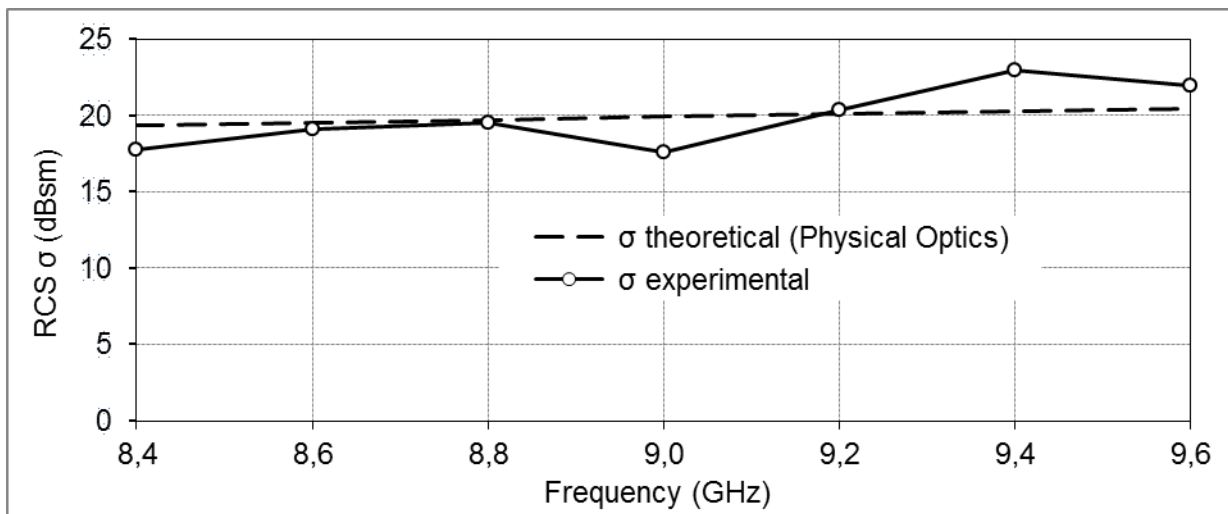


**FIGURE 4.** Comparison of theoretical and measured RCS values for the square plate target.

Based on the above considerations, the experimental RCS values from (7) are depicted in Fig. 4, along with the corresponding theoretical (physical optics) values given by (1).

A noteworthy agreement between experimental and theoretical RCS values is thus achieved, the discrepancy being about +2.7 dB at worst. In particular, the experimental RCS values appear consistent with the well-known upward trend of the theoretical RCS values with frequency.

## CONCLUSIONS

Application of the CW-nulling technique was tested in an unfavorable non-anechoic environment, using simple waveguide equipment, a general purpose scalar SA and several legacy

or COTS microwave signal sources, for frequencies in the X-band. A very inexpensive phase-locked YTO source was found adequate to achieve low levels of residual echo power after nulling, within 20 dB of the system noise floor, and corresponding levels of isolation between transmitter and receiver between 80 and 90 dB (depending on the test frequency). The average detection mode and the trace averaging function of the SA were helpful to reducing the residual echo. Further calibration measurements, with a conducting square plate target at normal incidence, allowed simple and straightforward estimation / verification of its RCS within 3 dB of the accepted physical optics values across the whole range of frequencies tested, even though the unwanted background echo signal was well above the wanted target return.

Notwithstanding limitations of the dynamic range and the uncertainty of measurements, these findings suggest the possibility of obtaining reasonable RCS estimates (probably with the exception of directions around target nulls) for a variety of targets, provided the target return levels are adequately high and, of course, the target dimensions are appropriate for the indoor test range and meet the far-field criterion. Further canonical target geometries could be studied this way. Larger targets could also be tested at appropriate frequencies via the dimensional scaling technique. Use of the present instrumentation for outdoor range measurements might also be explored by appropriate modifications (such as adding an output amplifier unit etc.) In such a scenario, results of previous computational work to model complex targets [11] might be considered for comparison purposes.

Several prospective improvements to the experimental setup and instrumentation are of interest and may be achieved at relatively low cost, notably replacement of the phase-locked YTO with an even stabler synthesized source (or just substitution of the onboard reference TCVCXO with a higher quality one), as well as background echo reduction by even a limited quantity of absorbers inserted into carefully selected locations within the test range.

## REFERENCES

1. *IEEE Recommended Practice for Radar Cross-Section Test Procedures*, IEEE Std 1502-2007, IEEE Antennas and Propagation Society, 2007.
2. E.F. Knott, *Radar Cross Section Measurements*, Van Nostrand Reinhold, 1993.
3. G.T. Ruck, D.E. Barrick, W.D. Stuart, C.K. Krichbaum, *Radar Cross Section Handbook*, Plenum Press, 1970.
4. R.G. Kouyoumjian, "The Calculation of the Echo Areas of Perfectly Conducting Objects by the Variational Method", Ph.D. Dissertation, Ohio State University, 1953.
5. J.N. Hines and T.E. Tice, "On Investigation of Reflection Measuring Equipment", Antenna Laboratory, Ohio State University, Report No. 478-13, 1953.
6. <http://www.ke5fx.com/stellex.htm>
7. <https://www.qsl.net/ct1dmk/stellex.html>
8. C.A. Balanis, *Antenna theory: analysis and design*, 2nd ed., John Wiley & Sons, 1997.
9. *Fundamentals of RF and Microwave Power Measurements*, Application Note 64-1, Hewlett Packard Co., 1977 (revised 1978).
10. *Fundamentals of RF and Microwave Power Measurements*, Application Note 64-1C, Agilent Technologies Co., 2001.
11. P. Frangos, E. Boulougouris, S. Pintzos and I. Aliferis, "Calculation of the Radar Cross Section of complex radar targets using high frequency electromagnetic techniques", International Conference on Electromagnetics in Advanced Applications (ICEAA '99), September 13 - 17, 1999, Torino, Italy.